Computerized Medical Imaging and Graphics 37 (2013) 394–402

Contents lists available at ScienceDirect

Computerized Medical Imaging and Graphics

journal homepage: www.elsevier.com/locate/compmedimag

Simple hybrid method for fine microaneurysm detection from non-dilated diabetic retinopathy retinal images

Akara Sopharak[a,*], Bunyarit Uyyanonvara[b,1], Sarah Barman[c]

[a] Faculty of Science and Arts, Burapha University, Chanthaburi Campus, 57 Moo 1, Kamong, Thamai, Chanthaburi 22170, Thailand
[b] Department of Information Technology, Sirindhorn International Institute of Technology (SIIT), Thammasat University, 131 Moo 5, Tiwanont Road, Bangkadi, Muang, Pathumthani 12000, Thailand
[c] Faculty of Computing, Information Systems and Mathematics, Kingston University, Penrhyn Road, Kingston upon Thames, Surrey KT1 2EE, UK

ARTICLE INFO

Article history:
Received 7 December 2012
Received in revised form 19 May 2013
Accepted 23 May 2013

Keywords:
Diabetic retinopathy
Microaneurysms
Naive Bayes classifier

ABSTRACT

Microaneurysms detection is an important task in computer aided diagnosis of diabetic retinopathy. Microaneurysms are the first clinical sign of diabetic retinopathy, a major cause of vision loss in diabetic patients. Early microaneurysm detection can help reduce the incidence of blindness. Automatic detection of microaneurysms is still an open problem due to their tiny sizes, low contrast and also similarity with blood vessels. It is particularly very difficult to detect fine microaneurysms, especially from non-dilated pupils and that is the goal of this paper. Simple yet effective methods are used. They are coarse segmentation using mathematic morphology and fine segmentation using naive Bayes classifier. A total of 18 microaneurysms features are proposed in this paper and they are extracted for naive Bayes classifier. The detected microaneurysms are validated by comparing at pixel level with ophthalmologists' hand-drawn ground-truth. The sensitivity, specificity, precision and accuracy are 85.68, 99.99, 83.34 and 99.99%, respectively.

1. Introduction

Diabetic retinopathy (DR) is the commonest cause of vision loss, and it prevalence is rising to 4.4% of the global population by 2030 [1]. In order to prevent the risk of blindness, diabetes patients need to have eye screening each year. It is time consuming and need an expert on the screening process. However with a large number of patients, the number of ophthalmologists is not sufficient to cope with all patients, especially in rural areas or if the workload of local ophthalmologists is substantial. Therefore the automated computer system can help ophthalmologists to screen the patients more efficiently.

Microaneurysms (MAs), are focal dilations of retinal capillaries and appear as small round dark red dots. There are four stages used for grading DR, grade 0 (no DR), grade 1 (mild), grade 2 (moderate) and grade 3 (severe). Each grade is classified by an appearance and number of microaneurysms and hemorrhage as shown in Table 1. Example of grade 0 and grade 1 DR are shown in Fig. 1(a) and (b). They appeared at the earliest clinically localized characteristic of DR, their detection would help to early treatment and prevent the blindness. It is difficult to detect MA because their pixels are similar to that of blood vessels. MA is hard to distinguish from noise or background variations because it has typically low contrast. In this paper we concentrate on MA detection as the earliest clinically localized characteristic of DR [2].

Previously published methods for MA detection have work on fluorescein angiographies or color images taken on patients with dilated pupils in which the MA and other retinal features are clearly visible. The quality of non-dilated pupil retinal images will be worse and it greatly affects the performance of the mentioned algorithms. The detection method proposed by Spencer et al. [3], Cree et al. [4] and Frame et al. [5] employ a mathematical morphology technique to segment MA within fluorescein angiograms. Top-hat operations based on linear structuring elements at a range of different inclinations are used. Vessel is removed but MAs of smaller diameter than the length of the structuring elements are retained. Gardner et al. [6] use a back propagation neural network on sub-images (20×20 or 30×30 pixel windows). The network is trained to identify the presence of vessels, exudates and hemorrhages (or MAs). They classify the regions of MA without extraction and localization. Sinthanayothin et al. [7] propose an automated system of detection of diabetic retinopathy using recursive region growing segmentation (RRGS). Vessels are detected by means of a multilayer perceptron neural network in which inputs are derived from a principle component analysis of the image and the edge detection. Then the objects remained after removal of vessels is assigned as MA. The

* Corresponding author. Tel.: +66 39 310 000; fax: +66 39 310 128.
E-mail addresses: akara@buu.ac.th (A. Sopharak), bunyarit@siit.tu.ac.th (B. Uyyanonvara), s.barman@kingston.ac.uk (S. Barman).
[1] Tel.: +66 2501 3505; fax: +66 2501 3524.

0895-6111/$ – see front matter © 2013 Elsevier Ltd. All rights reserved.
http://dx.doi.org/10.1016/j.compmedimag.2013.05.005

validation is done on 10×10 pixel grids not for individual images. Usher et al. [8] employ a combination of recursive region growing (RRG) and adaptive intensity thresholding (AIT) to detect candidate lesion regions. Candidate dark lesion is extracted to quantify numerically size, shape, hue and intensity. And a neural network is used for classification. Walter et al. [9] propose a method based on diameter closing and kernel density estimation for automatic classification. All candidate MA is detected by diameter closing and thresholding. Then 15 features are extracted for classification relies on kernel density estimation with variable bandwidth based on size, shape, color and gray level image. Dupas et al. [10] use a diameter-closing to segment MA candidate regions and k-nearest neighbors (*k*NN) to classify MA. The features based on size, contrast, circularity, gray-scale level and color are used. Niemeijer et al. [11] combine prior works by Spencer et al. [3] and Frame et al. [4] with a detection system based on pixel classification and new features are proposed. The top-hat transform is used for vessel detection. The total features set contain 68 features. A *k*NN classifier is used in the final step. Zhang et al. [12] use multi-scale correlation coefficients (MSCF). They detect pixels which are candidates of the MA using MSCF and fine MA using features classification. Gaussian kernels with five different scales are used. The sigmas of the Gaussian function are 1.1, 1.2, 1.3, 1.4 and 1.5. Thresholding is then applied in order to determine the number of MA candidates and region growing based algorithms are applied to allow a fit to the true MA size.

This paper has focused on automatic MA detection on images acquired without pupil dilation. A simple hybrid method is proposed. A preliminary MA detection system is published using a set of optimally adjusted morphological operators [13,14]. In order to improve the performance of MA detection, fine segmentation enhancement using naive Bayes classifier is combined. Our methodology is described in Section 2. In Section 3, the results of experiment are reported. Finally, the discussion and conclusion are present in Sections 4 and 5.

Table 1
Grading of diabetic retinopathy.

DR stage	
Grade 0 (no DR)	MA = 0 and H = 0
Grade 1 (mild)	$1 \leq$ MA ≤ 5 and H = 0
Grade 2 (moderate)	$5 <$ MA < 15 or $0 <$ H ≤ 5
Grade 3 (severe)	MA ≥ 15 or H > 5

MA: microaneurysm; H: hemorrhage.

2. Methods

All digital retinal images are taken from patients with non-dilated pupils using a KOWA-7 non-mydriatic retinal camera with a 45° field of view and taken at Thammasat University Hospital. The images are stored in JPEG image format files (.jpg) with lowest compression rates. The image size is 752×500 pixels at 24 bits per pixel. In Section 2.1, the preprocessing step includes noise removal, contrast enhancement and shade correction is described. Exudates and vessel are eliminated as described in Section 2.2. Section 2.3, candidate MAs are detected by using a set of optimally adjusted mathematical morphology. Section 2.4 explains the features we extract from each pixel in a retinal image. Finally, a fine MA detection is applied using the naive Bayes classifier in order to get an improvement in results as described in Section 2.5. The overall procedure of MA detection is shown in Fig. 2.

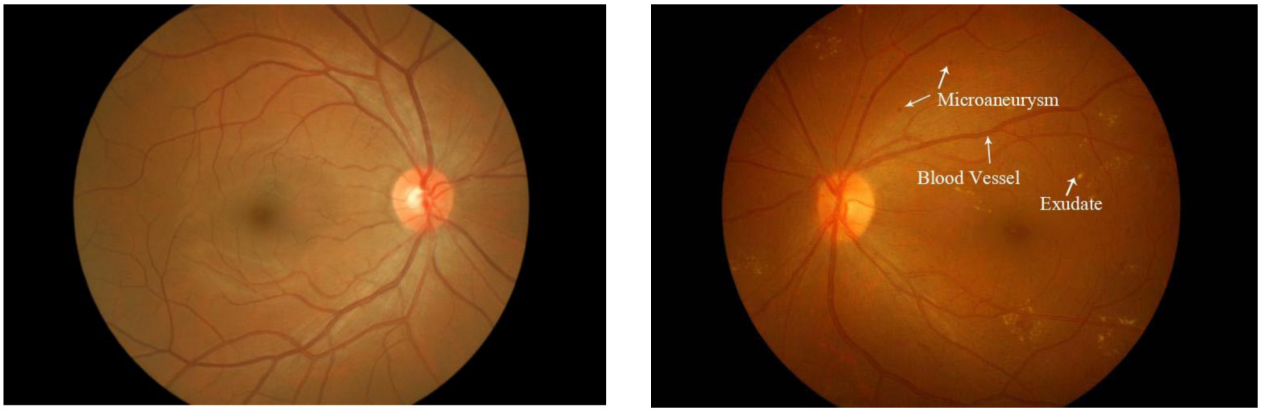

Fig. 1. Diabetic retinopathy image (a) grade 0 and (b) grade 1.

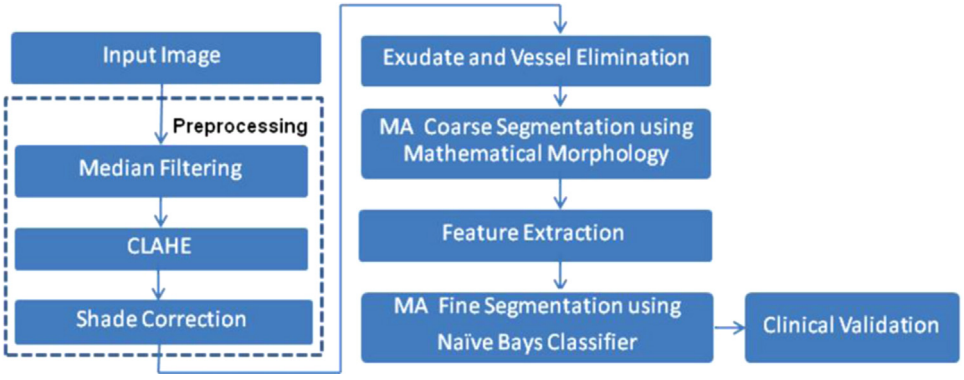

Fig. 2. Procedure of microaneurysm detection.

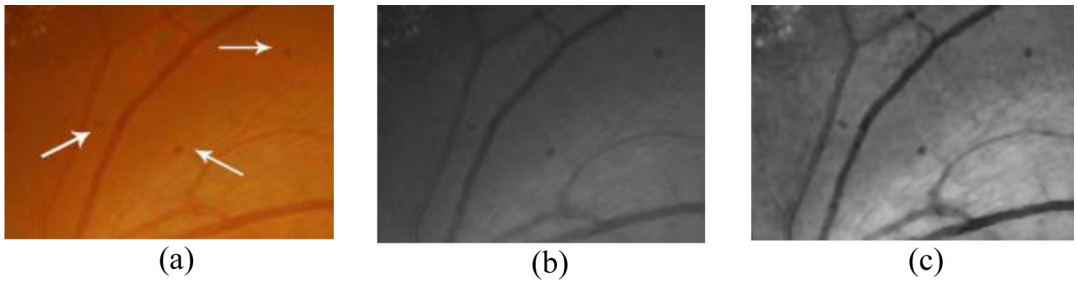

Fig. 3. Closeups of microaneurysm (a) original RGB image, (b) green plane and (c) shade corrected image.

2.1. Preprocessing

The quality of a retinal image has an impact on the performance of lesion detection algorithms. There are many factors that can cause an image to be of poor quality such as low contrast, noise, non-uniform illumination, variation in light reflection and diffusion, difference in retinal pigmentation and differences in cameras. The preprocessing is an important step in order to attenuate such image variations and improve image quality. The green plane (f_g) of the original image in RGB color space is used as red lesins such as MA and blood vessels have the highest contrast with the background in this color space. A median filtering operation is applied on f_g to attenuate the noise before a Contrast Limited Adaptive Histogram Equalization (CLAHE) is applied for contrast enhancement [15]. A dark region (including noise and MAs) may dominate after contrast enhancement. To account for this, a shade correction algorithm is applied to the green band in order to remove slow background variation due to non-uniform illumination. A "shade corrected image" is an image that slow gradients in the background of original image are removed. A shade corrected image is accomplished by subtracting the image with a low pass filter, in this experiment, the result of a 35×35 median filter applied to the image to correct for background variation. Closeups MA on original RGB image, green plane image and shade corrected image are shown in Fig. 3(a)–(c), respectively.

2.2. Exudate and vessel elimination

We have to remove bright lesions such as exudates prior to the process because when they lie close together, small islands are formed between them and they can be wrongly detected as MAs. The morphological reconstruction method is used for exudate detection [14]. Compared to the method in reference [11], Niemeijer et al. proposed a bright lesion removal by setting all pixels with a positive value to zero. For our exudates method, a set of optimally adjusted morphological operators is used for exudate detection on diabetic retinopathy patients' non-dilated pupil. It also works well even on low-contrast images while Niemeijer et al. method works well only on dilated pupils in which the exudates are clearly visible.

Vessels are another element in the image that needs to be removed prior the MA detection since MA and vessels both appear in a reddish color and MAs cannot occur on vessels. Candidate vessels are detected by the difference between the image after closing operator and the filled-in small black dot image. The objects on the difference image which have size smaller than 10 pixels (size of a MA) are then removed. The vessel and exudate detected results are shown in Fig. 4.

2.3. MA coarse segmentation using mathematical morphology

The main purpose for coarse segmentation is to identify MA candidates in a retinal image. Retinal MAs are focal dilatations of retinal capillaries. They are discrete, localized saccular distensions of the weakened capillary walls and appear as small round dark red dots on the retinal surface. The diameter of a MA lies between 10 and 100 μm, but it always smaller then a diameter $\lambda < 125$ μm [2,3]. In our image set of size 752×500 pixels, the size of a MA is about 10 pixels.

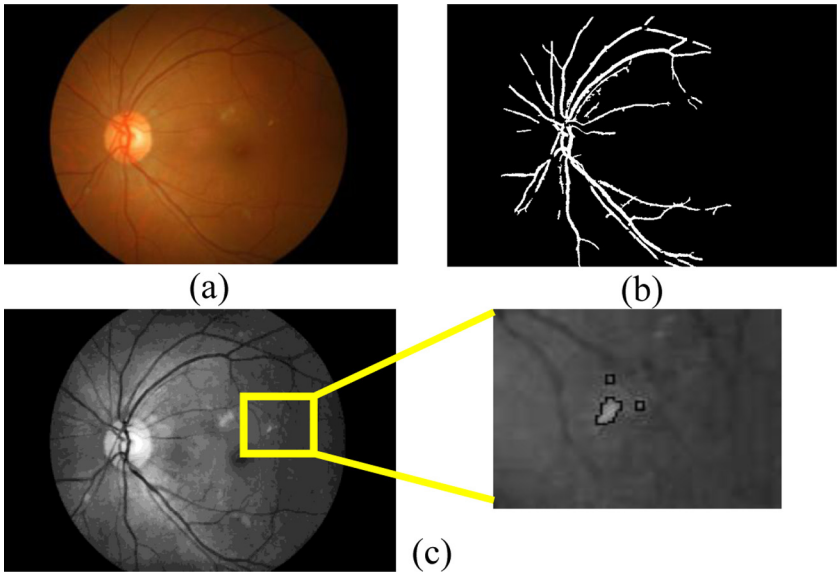

Fig. 4. Vessel and exudates detection (a) original RGB image, (b) vessel detected and (c) exudate detected.

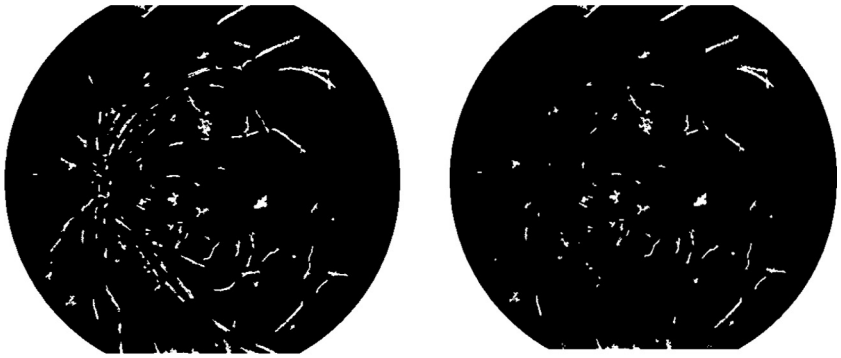

Fig. 5. Candidate microaneurysm detection (a) extended-minima transform image (b) image after removal of vessels and exudates.

Extended-minima transform is the region minima of h-minima transform. It is a kind of thresholding operation which will bring most of the valleys to zero. The h-minima transform suppresses all the minima in the intensity image whose depth is less than or equal to a predefined threshold. The output image is a binary image with the white pixels represents the regional minima in the original image. Regional minima are connected sets of pixels with the same intensity value, whose external boundary pixels all have a higher value. An 8-connected neighborhood is used [16]. We used this method for coarse segmentation to identify MA candidates.

From Ref. [9], Walter et al. proposed a method based on diameter closing and kernel density estimation for automatic classification. The mean of the diameter closing is applied for candidate MA detection. The associated top-hat transform is then used to eliminate candidates located on tortuous vessels and finally threshold is also needed to extract the candidates.

A preprocessed retinal image is used as preliminary image for MA detection. The extended-minima transform is applied to the shade corrected image (f_{sc}) image with gray levels in the range [0,1]. The output image f_E is a binary image with the white pixels represent the regional minima in the original image. The extended minima transform on the f_{sc} image with threshold value α_2 ($\alpha_2 = 0.05$ is used) is shown in Eq. (1).

$$f_E = EM(f_{sc}, \alpha_2) \tag{1}$$

where f_E is the output image and f_{sc} is the shade corrected image.

The selection of threshold is very important where the higher value of α_2 will lower the number of regions and a lower value of α_2 will raise the number of regions. A slight change in threshold value can cause the method either over-segment or under-segment the MA. α_2 is varied and tested in order to assess the algorithm performance in an experiment. The parameter is varied as follows:

$$\alpha_2 \in \{0.01, 0.03, 0.05, 0.07, 0.09\}$$

The parameter in this proposed method is set using the values that gave highest sensitivity and specificity in the previous experiment. The experiment showed that the value of $\alpha_2 = 0.05$ give a good balance between the number of detected MAs and the number of detected spurious objects.

The previous detected exudates and vessels are removed from the resulting image as shown in Eq. (2). The result is shown in Fig. 5.

$$f_{VE\_removed} = f_E - f_{vesselT} - f_{ex} \tag{2}$$

where f_{vessIT} is the vessel detected image and f_{ex} is the exudate detected image.

2.4. Feature extraction

We asked ophthalmologists how they identify MA in an image so that our feature extraction would reflect ophthalmologists' expertise. We found that intensity, color, size, shape and texture are the most important features they consider.

Niemeijer et al. [11] combine Spencer–Frame features with new proposed features. In total 68 features are used while Zhang et al. [12] apply 31 features on MA classification. A number of features should not be too large, because of the curse of dimensionality, but should contain enough information to detect MAs. A large number of features can be very time-consuming. With the concern on this point, we attempt to mimic ophthalmologist expertise by extracting relevant and significant features. Then 18 features are used to distinguish MA pixels from non-MA pixels (pixels that might be the candidate of the MA but not the real MA pixels).

As an initial set of candidate per-pixel features, we selected 18 features and used them as input for our classifier. A general motivation and an explanation of the motivation for each feature is explained in this section.

1. The pixel's intensity value of shade corrected image (I_{sc}).
2. The pixel's intensity value of green band image after preprocessing (I_g).
3. *The pixel's hue*. Hue characterized chrominance or color information, which should distinguish MAs from non-MAs.
4. *The standard deviation of shade corrected image*. A window size of 15×15 is used.
5. *The standard deviation of green band image after preprocessing*. A window size of 15×15 is used.
6. *Six Difference of Gaussian (DoG) filter responses*. The DoG filter subtracts one blurred version of an original image from another blurred version of the image [17]. We convolve with seven different Gaussian kernels with standard deviations of 0.5, 1, 2, 4, 8, 16, and 32. We use DoG1, DoG2, DoG3, DoG4, DoG5 and DoG6 to refer to the features obtained by subtracting the image at scale $\sigma = 0.5$ from scale $\sigma = 1$, scale $\sigma = 1$ from $\sigma = 2$, scale $\sigma = 2$ from $\sigma = 4$, scale $\sigma = 4$ from $\sigma = 8$, scale $\sigma = 8$ from $\sigma = 16$, and scale $\sigma = 16$ from $\sigma = 32$, respectively.
7. The area of the candidate MA.
8. The perimeter of the candidate MA.
9. The eccentricity of the candidate MA.
10. The circularity of the candidate MA.
11. The mean intensity of the candidate MA on shade corrected image.
12. The mean intensity of the candidate MA on green band image.
13. The ratio of the major axis length and minor length of the candidate MA.

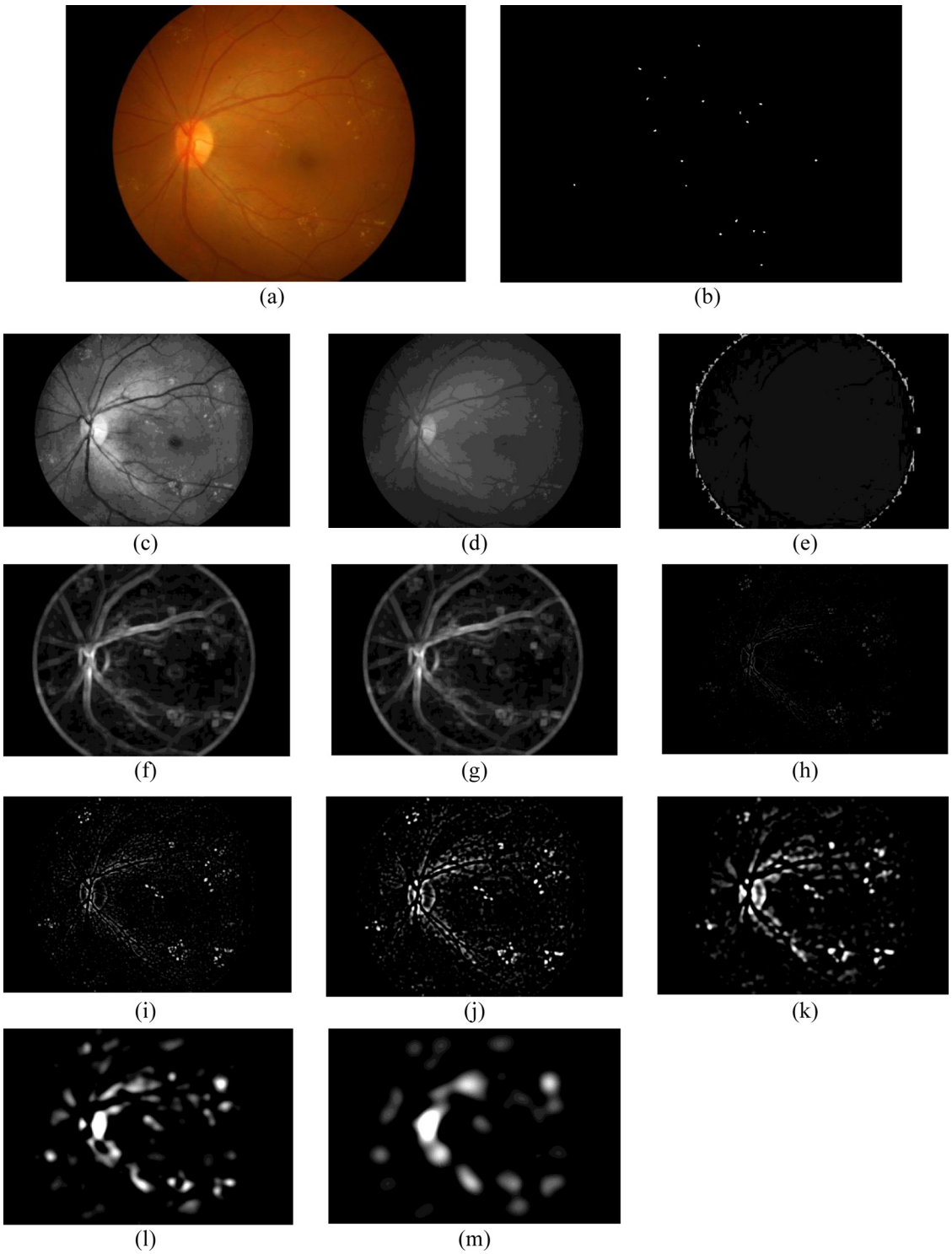

Fig. 6. Examples of some feature extracted, (a) original image, (b) candidate MA, (c) pixel's intensity of shade corrected image, (d) pixel's intensity of green band image, (e) pixel's hue, (f) standard deviation of shade corrected image, (g) standard deviation of green band image, (h) DoG1, (i) DoG2, (j) DoG3, (k) DoG4, (l) DoG5, (m) DoG6.

Before feature selection or classification, we z-scale (transform to a mean of 0 and a standard deviation of 1) all 18 features using the statistics of each feature over the training set.

2.5. MA fine segmentation using naive Bayes classsifier

The result from the previous section is a rough estimation of the MA. In order to get a better result, a fine segmentation using naive Bayes classifier is applied in this step.

According to the usefulness and efficiency, Bayesian networks have been used in different areas of computer vision and image processing. Bayesian networks have also become an important formalism for medical decision support systems. The naive Bayes classifier [18–20] uses the principle of Bayesian maximum a posteriori (MAP) classification: measure a finite set of features $\mathbf{x} = (x_1, \ldots, x_n)$ then select the class

$$\hat{y} = \underset{y}{\operatorname{argmax}} P(y|x)$$

where

$$P(y|x) \propto P(x|y)P(y) \quad (3)$$

$P(\mathbf{x}|y)$ is the likelihood of feature vector $\mathbf{x}$ given class y, and $P(y)$ is the priori probability of class y. Naive Bayes assumes that the features are conditionally independent given the class:

$$P(x|y) = \prod_i P(x_i|y)$$

We estimate the parameters $P(x_i|y)$ and $P(y)$ from training data.

After z-scaling, all of our features x_i are continuous, but the simple version of naive Bayes just described requires discrete features, so we perform unsupervised proportional k-interval discretization as implemented in Weka [21]. The technique uses equal-frequency binning, where the number of bins is the square root of the number of values. After discretization, the conditional probability tables are obtained by simply counting over the training set.

In our experiment, our classification is pixel-based. Each pixel is classified as MAs or non-MAs independently from its neighbor. Features of each candidate pixel are extracted. Then, extracted features are entered as input to the naive Bayes classifier. The naive Bayes classifier is trained with sets of input features and correct class labels. A class label of 1 is assigned to the corresponding output unit when a training sample belongs to MAs, and 0 is assigned to the non-MAs output units. After training, the class of the unit with the maximum value is determined to be the corresponding class to which an unknown sample belongs.

The example image of candidate MA after segmentation is shown in Fig. 6(b) and the value of feature extracted from candidate MA pixel are used as the input to the classifier. Fig. 6 shows examples of some feature extracted from the image.

3. Results

Data sets of 80 non-dilated retinal images are performed preprocessing on a PC with a P-II 1.6 GHz CPU, 512 Mb RAM using the MATLAB program. A set of 40 retinal images is used as a training set, 30 retinal images with MA and 10 normal retinal images are used as a testing set. For each image in the training set, we compute the features for every MA pixel then randomly selected and computed features from an equal number of non-MA pixels. The two sets of examples formed our training set.

In our experiment, the classification is pixel-based. Even though the number of images seems small, the actual training and testing sample size that we extracted from them are in fact quite large. We thus obtain 4546 samples, 2273 examples of MA pixels and 2273 examples of non-MA pixels, for training. From our test images, we use the 1982 MA pixels and 5,638,018 non-MA pixels as a testing set. For test set, the number of non-MA pixels will always larger than number of MA pixels due to the background and other objects pixels. A Weka data mining software running on a standard PC for feature discretization and naive Bayesian classification is used. The running time per image of our proposed method is about 1 min.

The performance of our technique is evaluated quantitatively by comparing the resulting extractions with ophthalmologists' hand-drawn ground-truth images pixel by pixel. In order to facilitate the experts to produce a ground-truth image, a first draft of ground-truth image is created by us. We mark the very obvious MA pixels, pixel by pixel, using a photo manipulation program with one color. Then, this first draft image is shown to two expert ophthalmologists together with the original image. The ophthalmologists then make some changes by adding some missing MA pixels and/or removing some misunderstood non-MA pixels until it is agreed by both experts.

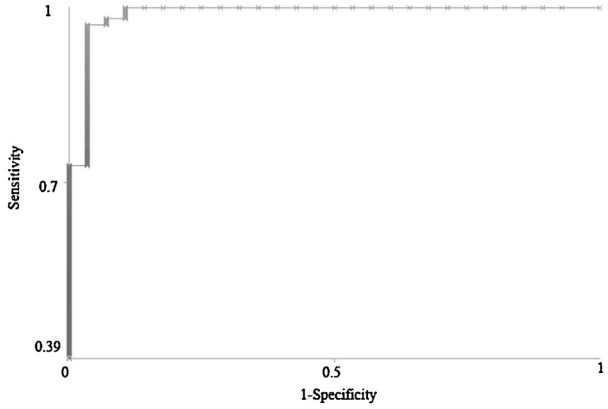

Fig. 7. ROC curve of purposed method.

As a simple baseline for comparison, nearest neighbor classifier with Euclidean distance is used. The nearest neighbor classifier simply classifies a test instance with the class of the nearest training instance according to some distance measure. Sensitivity and specificity are chosen as our measurement of accuracy of the algorithms at the pixel level. Not only does this evaluation mechanism show how accurate our detection is, it also shows how inaccurate our detector can be. Precision is the percentage of detected pixels that are actually MAs. Accuracy is the overall per-pixel success rate of the classifier. This pixel-based evaluation considers four values, namely true positive (TP), a number of MA pixels correctly detected, false positive (FP), a number of non-MA pixels which are detected wrongly as MA pixels, false negative (FN), a number of MA pixels that are not detected and true negative (TN), a number of non-MA pixels which are correctly identified as non-MA pixels. From these quantities, the sensitivity, specificity, precision and accuracy are computed using Eq. (4) through Eq. (7).

$$\text{Sensitivity} = \frac{TP}{TP + FN} \quad (4)$$

$$\text{Specificity} = \frac{TN}{TN + FP} \quad (5)$$

$$\text{Precision} = \frac{TP}{TP + FP} \quad (6)$$

$$\text{Accuracy} = \frac{TP + TN}{TP + FP + FN + TN} \quad (7)$$

Sensitivity, specificity, precision and accuracy in this experiment are 85.68, 99.99, 83.34 and 99.99%, respectively. For normal retinal image detection, the specificity is 89%. The sensitivity cannot be calculated in which TP and FN values are all zero due to no MA in ground-truth images. Sensitivity and specificity are used to create receiver operator characteristic (ROC) curves as shown in Fig. 7. From the ROC curve, the optimal threshold is the subjective point. Any increase in sensitivity will be accompanied by a decrease in specificity. The system performance is evaluated by determining the sensitivity and specificity of the algorithm at the optimal threshold.

A comparison of average result from mathematical morphology from our previous paper [13], combined mathematical morphology with naive Bayes classifier and nearest neighbor is shown in Table 2. Comparing with baseline algorithm, the results indicate that our purposed method performs better in specificity, precision and accuracy than nearest neighbor. Fig. 8 displays the comparison of MA detection from mathematical morphology, result of fine-tuned segmentation using naive Bayes classifier and ground truth image. The numbers of MAs are also counted for automated grading

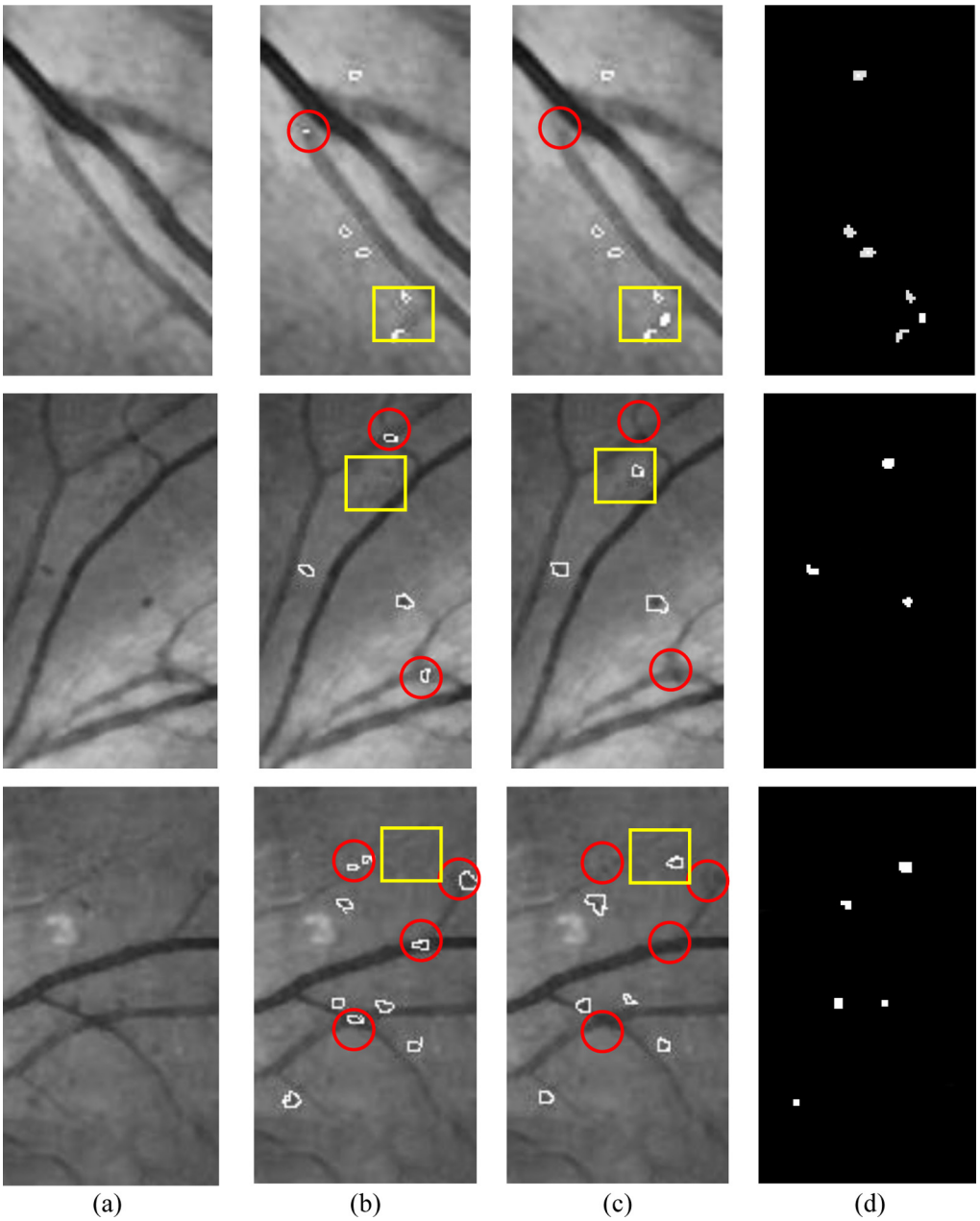

Fig. 8. Comparison of microaneurysm detection results. (a) Original image, (b) result from morphology, (c) result from naive Bayes classifier and (d) ground truth image.

of the severity of the DR. The average accuracy on grading DR stage is 88.31% as shown in Table 3.

From our previous MA detection experiment using only mathematical morphology, there are some missing true MA pixels and some false MA detection on faint blood vessels appears. This experiment has shown that the proposed method could cope this problem. It could detect those misclassified MA (shown in yellow square box in Fig. 8(c)) and reduces the false MA (shown in red circle in Fig. 8(c)).

Table 2
Comparison of average result from mathematical morphology, naive Bays classifier and nearest neighbor.

Method	Se (%)	Sp (%)	Pr (%)	Accuracy (%)
Morphology	81.61	99.99	63.76	99.98
Morphology + naive Bayes classifier	85.68	99.99	83.34	99.99
Nearest neighbor	87.15	96.60	65.43	96.50

Se: sensitivity, Sp: specificity and Pr: precision.

4. Discussion

In this paper we proposed the method of automatic MA detection using hybrid approach. Combined of mathematical

Table 3
Performance of grading diabetic retinopathy stage.

DR stage	MA's detected		No. of images	Accuracy (%)
	No	Yes		
Grade 0 (no DR)	13	2	15	86.68
Grade 1 (mild)	1	14	15	93.33
Grade 2 (moderate)	1	7	8	87.50
Grade 3 (severe)	1	6	7	85.71
Average				88.31

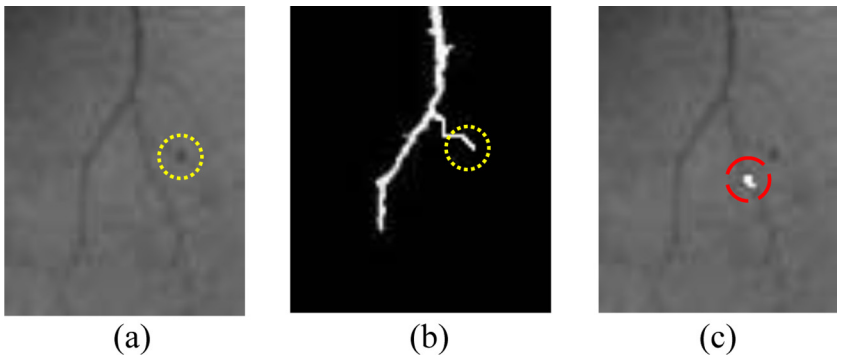

Fig. 9. Example of false microaneurysm detection. (a) Image with true MA, (b) blood vessel detected and (c) MA detected on faint blood vessels.

morphology and naive Bayesian classifier is investigated. Mathematical morphology is a simple method and computationally low cost but it does not achieve good sensitivity. The result shows that sensitivity, precision and accuracy values increase when the naive Bayes classifier is combined. The British Diabetic Retinopathy Working Group [22] recommends a minimum sensitivity of 80% and specificity of 95%, the result from our system is well above that.

*k*NN is based on a distance function. A number of *k* has to be defined. The weakness of *k*NN is that it could not handle high number of dimensions well. The naive Bayes classifier is a simple but effective Bayesian classifier for vector data that assumes that attributes are independent given the class. The naive Bayes classifier benefits on handle high number of dimensions of independent features. The independent features are statistically independent. Due to limitations on the amount of diabetic retinopathy retinal images with MA, number of lesions is small. In our experiment, pixel-based classification is used. The benefit of using each pixel in the training stage is a relatively large number of training data with labeled data and that is why the naïve Bayes classifier is preferred.

This system intends to help the ophthalmologists in the diabetic retinopathy screening process for detecting the symptoms faster and more easily. The results demonstrated here indicate that automated diagnosis of diabetic retinopathy based on hybrid approach can be very successful in detecting MA. It is not a final-result application but it can be a preliminary diagnosis tool or decision support system for ophthalmologists. Human ophthalmologists are still needed for the cases where detection results are not very obvious.

There are some incorrect MA detections which are caused by the artifacts, too small MA, too blurred MA, faint blood vessels which cannot detected/removed or MA that appear very faint. There are some missing MAs located next to or nearby blood vessels which are removed as wrongly detected as blood vessels. They are also faint blood vessels which are not removed in vessel detection step; MA could be wrongly detected on those vessels. For example, as shown in Fig. 9(b) on yellow circle mark, true MA is wrongly detected as vessel and removed in prior step. Fig. 9(c) on red circle mark shows that faint blood vessels can be incorrectly detected as MA. The results of MA detection depend on the success of vessel detection. A main weakness of the algorithm arises from the fact that the algorithm depends on vessel detection. This indicates the further necessity of improving the robustness of this task. Hemorrhages detection could be also added to the system in order to increase its ability to verify the degree of diabetic retinopathy.

5. Conclusion and future work

In this paper we proposed real-time and simple hybrid approach based on mathematic morphology and naive Bayes classifier to detect MA from non-dilated retinal image. This consisted of coarse segmentation using mathematic morphology and fine segmentation using naive Bayes classifier. Eighteen input features based on the characteristics of MA are selected. Blood vessel and exudates are also removed from all features in order to prevent misclassification. The running time per image is about 1 min on a PC with a P-II 1.6 GHz CPU and 512 MB RAM. The performance of the algorithm is measured against ophthalmologists' hand-drawn ground-truth. Sensitivity, specificity, precision and accuracy are used as the performance measurement of MA detection because they combine true positive and false positive rates. Accuracy values are also used to evaluate the system. The system also provided ophthalmologists with the number of MAs for grading the DR stage. We conclude that the proposed approach is effective yet simple and fast for MA detection and localization of DR stage. The system intended to help the ophthalmologists in the diabetic retinopathy screening process to detect symptoms faster and more easily. The proposed techniques work effectively even on a poor computing system.

Future work will address an issue of improving the sensitivity by improving the results of other tasks, such as the detection of the blood vessels, and also try to localize faint and small MA. With a numbers of features, the naive Bayes classifier is computationally expensive during training process. Reducing feature dimension would be help to decrease the training time. A data set should be expanded and the system should be clinically tested as a practical aid to help ophthalmologists screen patients for diabetic retinopathy symptoms quickly and easily. In addition, other techniques should be tested and compared to the system in order to get a better result.

Additionally, ground-truth creation may also be done solely by expert ophthalmologists in order to reduce authors' bias and the results from that test set may be used to compare with the current one.

Conflict of interest

No conflict of interest.

Acknowledgements

This research is funded by the Burapha University, Chanthaburi Campus and National Research University Project of Thailand Office of Higher Education Commission (Thammasat University).

References

[1] Wild S, Roglic G, Green A, Sicree R, King H. Global prevalence of diabetes: estimates for the year 2000 and projections for 2030. Diabetes Care 2004;27:1047–53.
[2] Massin P, Erginay A, Gaudric A. Retinopathie Diabetique. Elsevier, Editions scientifiques of medicales. Paris: Elsevier, SAS; 2000.
[3] Spencer T, Olson JA, McHardy KC, Sharp PF, Forrester JV. An image-processing strategy for the segmentation and quantification of microaneurysms in fluorescein angiograms of the ocular fundus. Comp Biomed Res 1996;29:284–302.

[4] Cree MJ, Olson JA, McHardy KC, Sharp PF, Forrester JV. A fully automated comparative microaneurysm digital detection system. Eye 1997;11:622–8.
[5] Frame AJ, Undrill PE, Cree MJ, Olson JA, McHardy KC, Sharp PF, et al. A comparison of computer based classification methods applied to the detection of microaneurysms in ophthalmic fluorescein angiograms. Comput Biol Med 1998;28:225–38.
[6] Gardner GG, Keating D, Williamson TH, Elliott AT. Automatic detection of diabetic retinopathy using an artificial neural network: a screening tool. Br J Ophthalmol 1996;80:940–4.
[7] Sinthanayothin C, Boyce JF, Williamson TH, Cook HL, Mensah E, Lal S, et al. Automated detection of diabetic retinopathy on digital fundus image. Diabet Med 2002;19:105–12.
[8] Usher D, Dumskyj M, Himaga M, Williamson TH, Nussey S, Boyce J. Automated detection of diabetic retinopathy in digital retinal images: a tool for diabetic retinopathy screening. Diabet Med 2004;21:84–90.
[9] Walter T, Massin P, Erginay A, Ordonez R, Jeulin C, Klein JC. Automatic detection of microaneurysms in color fundus images. Med Image Anal 2007;11:555–66.
[10] Dupas B, Walter T, Erginay A, Ordonez R, Deb-Joardar N, Gain P, et al. Evaluation of automated fundus photograph analysis algorithms for detecting microaneurysms, haemorrhages and exudates, and of a computer-assisted diagnostic system for grading diabetic retinopathy. Diabetes Metab 2010;36:213–20.
[11] Niemeijer M, van Ginneken B, Staal J, Suttorp-Schulten MS, Abramoff MD. Automatic detection of red lesions in digital color fundus photographs. IEEE Trans Med Imag 2005;24:584–92.
[12] Zhang B, Wu X, You J, Li Q, Karray F. Detection of microaneurysms using multi-scale correlation coefficients. Pattern Recogn Lett 2010;43:2237–48.
[13] Sopharak A, Uyyanonvara B, Barman S. Automatic microaneurysm detection from non-dilated diabetic retinopathy retinal images using mathematical morphological methods. IAENG J Comput Sci 2011;38:295–301.
[14] Sopharak A, Uyyanonvara B, Barman S, Williamson TH. Automatic detection of diabetic retinopathy exudates from non-dilated retinal images using mathematical morphology methods. Comput Med Imag Grap 2008;32:720–7.
[15] Gonzales RC, Woods RE. Digital image processing. New York: Addison-Wesley; 1993. p. 75–140.
[16] Soille P. Morphological image analysis: principles and applications. New York: Springer-Verlag; 1999. p. 170–1.
[17] Kenneth RS, John CR, Matthew J, Thomas JF, Michael WD. Difference of Gaussians Edge Enhancement [Online]; 2006, June 15. Available: http://micro.magnet.fsu.edu/primer/java/digitalimaging/processing/diffgaussians/index.html
[18] Friedman N, Geiger D, Goldszmidt M. Bayesian network classifiers. Mach Learn 1997;29:131–63.
[19] Richard OD, Peter EH, David GS. Pattern classification. 2nd ed. A Wiley-Interscience Publication; 2000. p. 20–83.
[20] Wang XY, Garibaldi J, Ozen T. Application of the fuzzy C-means clustering method on the analysis of non pre-processed FTIR data for cancer diagnosis. In: Proceeding of the International Conference on Australian and New Zealand Intelligent Information Systems (ANZIIS). 2003. p. 233–8.
[21] Witten IH, Frank E. Data mining: practical machine learning tools and techniques. 2nd ed. San Francisco: Morgan Kaufmann; 2005. p. 363–473.
[22] British Diabetic Association. Retinal photography screening for diabetic eye disease. London: British Diabetic Association; 1997.

Akara Sopharak received the B.Sc. and M.Sc. degrees in Computer Science from Burapha University and Mahidol University, Thailand, in 1998 and 2002 respectively. She received her Ph.D. in Information Technology from Sirindhorn International Institute of Technology, Thammasat University in 2009. She is currently lecturer at Faculty of Science and Arts, Burapha University, Chanthaburi Campus. Her research interests include medical image processing.

Bunyarit Uyyanonvara is currently an associate professor in Information Technology at Sirindhorn International Institute of Technology, Thammasat University. He recieved his B.Sc. (1st Class Honors) in Science from Prince of Songkhla University in 1995 and his Ph.D. in Medical Image Processing from King's College, University of London in 2000.

Dr Barman's qualifications include a B.Sc. in Physics from Essex University, an M.Sc. in Applied Optics from Imperial College, University of London and a Ph.D. in Optical Physics from King's College, University of London. Since 2000, Dr Kingston University and is currently investigating medical imaging algorithms, based on her experience of image processing and optical modeling techniques for use on a range of ophthalmic images.